The Journal of Veterinary Medical Science

FULL PAPER

Laboratory Animal Science

High-fat/high-sucrose diet-induced renal changes in obese diabetic mice: a comparison with *db/db* and KK-Ay mice

Chika OKI[1,2], Kinuko UNO[2], Tomohiko SASASE[1,2]*, Takahiro TSUTSUI[2], Keita SEKIGUCHI[3], Ayane YAMAGUCHI[3], Kouhei MANDAI[3], Masami SHINOHARA[4], Miki SUGIMOTO[2], Tatsuya MAEKAWA[3], Katsuhiro MIYAJIMA[3], Takeshi OHTA[2]

[1)]Biological/Pharmacological Research Laboratories, Takatsuki Research Center, Central Pharmaceutical Research Institute, Japan Tobacco Inc., Osaka, Japan
[2)]Laboratory of Animal Physiology and Functional Anatomy, Graduate School of Agriculture, Kyoto University, Kyoto, Japan
[3)]Department of Nutritional Science and Food Safety, Faculty of Applied Biosciences, Tokyo University of Agriculture, Tokyo, Japan
[4)]Tokyo Animal & Diet Dept, CLEA Japan Inc., Tokyo, Japan

ABSTRACT. Many genetic and environmental factors are involved in the development and progression of diabetic kidney disease (DKD), and its pathology shows various characteristics. Animal models of DKD play an important role in elucidating its pathogenesis and developing new therapies. In this study, we investigated the pathophysiological features of two DKD animal models: *db/db* mice (background of hyperglycemia) and KK-Ay mice (background of hyperinsulinemia). Male and female mice were fed a high-fat/high-sucrose (HFS) diet for eight weeks. Two mouse models fed the HFS diet showed increases in urinary protein, kidney weight, and glomerular size, but these changes were pronounced in KK-Ay mice. Pathological examination revealed tubulointerstitial fibrosis in KK-Ay mice fed the HFS diet, but not in *db/db* mice. In addition, fat accumulation was observed in the macula densa of *db/db* mice and in the glomeruli of KK-Ay mice fed with the HFS diet. In conclusion, an HFS diet exacerbates renal lesions with tubulointerstitial fibrosis in KK-Ay mice, and KK-Ay mice fed an HFS diet are expected to be useful as a DKD model.

KEYWORDS: *db/db* mice, diabetic kidney disease, high-fat/high-sucrose diet, KK-Ay mice

J Vet Med Sci
87(2): 138–146, 2025
doi: 10.1292/jvms.24-0313

Received: 27 August 2024
Accepted: 25 November 2024
Advanced Epub:
11 December 2024

INTRODUCTION

With the increasing global prevalence of diabetes mellitus (DM), the number of patients with microvascular complications associated with DM is increasing rapidly [2, 8]. Diabetic kidney disease (DKD) −also known as diabetic nephropathy and one of the most frequent diabetic microvascular complications−is the main cause of chronic kidney disease (CKD) and leads to the development of end-stage renal disease (ESRD) and cardiovascular disease [5, 10].

The pathology of DKD involves multifactorial interactions, including metabolic and hemodynamic factors driven by hyperglycemia and hypertension [19, 27]. Intensive glycemic control and blood pressure control delay the development and progression of DKD but cannot prevent it [5, 31]. There is no fundamental treatment for DKD, and there is still an unmet medical need.

Complex pathogenesis affects the glomeruli and tubules in DKD. Mesangial expansion, glomerular endothelial cell dysfunction, and loss of podocytes are observed in the glomeruli, and inflammation-driven interstitial fibrosis is observed in the tubules [10, 12]. Renal dysfunction is closely associated with the accumulation of extracellular matrix proteins, including collagen and fibronectin, leading to fibrosis. Tubulointerstitial fibrosis is thought to be a common pathway in CKD that ultimately leads to ESRD and death [9, 21, 25, 26, 33].

Animal models are essential for elucidating pathogenesis and developing new therapies, including potential drugs and biomarkers. In the present study, we used two obese diabetic mouse models: *db/db* and KK-Ay. The phenotypes of *db/db* mice include hyperphagia, obesity, and diabetes owing to spontaneous mutations in the abnormal splicing of leptin receptors [6, 22]. Hyperphagia and obesity in KK-Ay mice are caused by multiple genes, and induction of the A^y allele leads to hyperphagia by introducing different combinations

*Correspondence to: Sasase T: tomohiko.sasase@jt.com, Biological/Pharmacological Research Laboratories, Takatsuki Research Center, Central Pharmaceutical Research Institute, Japan Tobacco Inc., Takatsuki, Osaka 569-1125, Japan

of loci responsible for these traits [35, 36]. Both mouse models develop diabetes with hyperphagia due to impairment of anorectic activity; *db/db* mice are characterized by marked hyperglycemia, whereas KK-Ay mice are characterized by marked hyperinsulinemia [16, 40]. Since neither *db/db* mice nor KK-Ay mice fed a standard diet developed tubulointerstitial fibrosis, a common pathway for CKD [16], we investigated the pathological changes in two mouse models induced by high fat/high sucrose (HFS) feeding. In the fat-sugar interaction study, the high fat diet or the high sucrose diet causes fat accumulation and weight gain through different mechanisms, and each diet can be an exacerbating factor for the other [42]. Furthermore, compared to the high-fat diet, the HFS diet increased gut microbiota associated with insulin resistance, while decreasing gut microbiota that suppress inflammation, suggesting a worsening of diabetic complications including DKD [24].

MATERIALS AND METHODS

Animals

Male and female *db/db* and KK-Ay mice (CLEA Japan, Tokyo, Japan) were used in this study. C57BL/6J mice (CLEA Japan) were used as controls. At 6 weeks of age, each mouse was divided into the same two groups: a normal chow (NC) diet (CE-2; 3.4 kcal/g; CLEA Japan) and a HFS diet (14% fat and 25% sucrose, based on percentage of total calories, Quick Fat; 3.96 kcal/g; CLEA Japan). The mice were fed an NC or HFS diet from 6–14 weeks of age. The animals were housed individually in plastic cages in a room climate-controlled for temperature (24 ± 2°C), humidity (50 ± 10%), and lighting (10-hr dark/14-hr light cycle). In addition, they had free access to water. All the remaining animals were necropsied at 14 weeks of age. All experimental protocols and animals were used in strict compliance with the Kyoto University guidelines for animal experimentation (Animal Experiment Approval No. R3-107).

Biological parameters

Body weight, kidney weight, blood biochemical parameters such as serum glucose, insulin, triglyceride (TG), total cholesterol (TC), and creatinine levels, and urine biochemical parameters such as urine volume, urinary protein, and creatinine levels were measured at 14 weeks of age. Blood samples were collected from the abdominal vena cava under isoflurane anesthesia. The urine samples were collected for 8 hr in metabolic cages. Serum glucose, insulin, TG, TC, creatine, and urine creatinine levels were measured using respective product kits (Roche Diagnostics, Tokyo, Japan) and an automatic analyzer (Hitachi High-Tech, Tokyo, Japan). Serum insulin levels were measured using an enzyme-linked immunosorbent assay kit (Morinaga Institute of Biological Science, Yokohama, Japan). Urinary protein levels were measured using a commercial kit (Micro TP-Test Wako; Fujifilm Wako Pure Chemical, Osaka, Japan). Creatinine clearance (mL/hr·g) was calculated by dividing the urinary excretion for 8 hr of creatine by the serum creatinine levels and body weight.

Tissue sampling and histopathology

Dissections were performed at 14 weeks of age. The animals were euthanized by cervical dislocation after blood sample collection by exsanguination under isoflurane anesthesia. The kidneys were sampled for the measurement of mRNA expression and histopathology. Samples for mRNA analysis were stored in RNAlater (Sigma-Aldrich Japan, Tokyo, Japan) at −20°C until use. For pathological analysis, the kidneys were fixed in 10% neutral-buffered formalin immediately after collection. The tissues were paraffin-embedded by standard techniques and cut into 4-µm-thick sections. For histopathological evaluation and renal fibrosis analysis, tissue sections were stained with hematoxylin and eosin (HE) and Sirius red (SR) stain, respectively. The findings were graded from negative (−), very slight changes (±), slight (+), moderate (2+), and severe (3+). Abnormal findings in the tubules and tubulointerstitium were expressed as a percentage of the total area of the observation region, with 0% (−), less than 25% (±), 25–50% (+), 50–75% (2+), and 75% or more (3+). Furthermore, abnormal findings in the glomeruli were evaluated as the ratio of the number of abnormal glomeruli to the total number of glomeruli. Oil Red O staining was performed to investigate lipid accumulation in the male kidneys. Female frozen sections could not be used due to age-related deterioration.

The kidneys were fixed in 10% neutral formalin buffer, rinsed with tap water, dehydrated with a sucrose solution, and embedded in Tissue-Tek OCT compound. The embedded samples were sectioned (6-µm thick) using a cryostat (Leica Microsystems, Tokyo, Japan) and stained with Oil Red O (Nacalai Tesque, Kyoto, Japan). For this staining, 3 samples (NC group) and 5 (HFS group) of C57BL/6J mice, 5 (NC) and 4 (HFS) of *db/db* mice, 5 (NC) and 5 (HFS) of KK-Ay mice were used.

To measure glomerular size, one section per mouse was imaged under a light microscope (BX51, Olympus, Tokyo, Japan) using a 4× objective lens and analyzed using ImageJ (U.S. National Institutes of Health, Bethesda, MD, USA) [32]. The entire image of each section was stitched together using the stitching plugin in the ImageJ software [29] and unbiased counting frames with an area sampling fraction of 70%. The sizes of more than 50 glomeruli were measured in each animal. The profile of the glomeruli in the counted areas was traced manually using a polygon tool. The best-fit ellipse was determined for each glomerulus and the lengths of the major and minor axes were measured.

mRNA quantification

Total kidney RNA was extracted using Sepasol-RNA I Super G (Nacalai Tesque), according to the manufacturer's protocol. Reverse transcription was performed using the ReverTra Ace quantitative real-time PCR (qPCR) Master Mix (Toyobo, Osaka, Japan) to synthesize complementary DNA (cDNA). qPCR was performed using Thunderbird SYBR qPCR Mix (Toyobo). All procedures were performed according to the manufacturer's instructions. Gene expression was quantified using the following primers: transforming growth factor (TGF)-β forward: GCAACATGTGGAACTCTACCAGA, reverse: GACGTCAAAAGACAGCCACTCA, tissue

inhibitor of metalloproteinases 1 (TIMP-1) forward: AGGTGGTCTCGTTGATTTCT, reverse: GTAAGGCCTGTAGCTGTGCC, cyclophilin forward: TGGCTCACAGTTCTTCATAACCA, reverse: ATGACATCCTTCAGTGGCTTGTC. Cyclophilin was used as an internal control.

Statistical analysis

All values are expressed as the mean ± standard deviation (SD). Statistical analyses between groups were performed using a one-way ANOVA between strains or diets. Statistical significance was set at $P<0.05$.

RESULTS

Biological parameters

Changes in biological parameters are shown in Tables 1 and 2 (male) and Tables 3 and 4 (female). *db/db* and KK-Ay mice showed obesity, which was more pronounced in the HFS diet. Both diabetic mice showed hyperglycemia and KK-Ay mice showed hyperinsulinemia. Male KK-Ay mice fed the HFS diet exhibited more severe hyperglycemia compared to male KK-Ay mice fed the NC diet. KK-Ay mice fed the HFS diet exhibited more severe hyperinsulinemia compared with *db/db* mice fed the HFS diet, indicating strong insulin resistance in KK-Ay mice fed the HFS diet. Moreover, lipid abnormalities were observed in both diabetic mice, and hypercholesterolemia was enhanced by the HFS diet. Increases in urine volume and urinary protein levels were observed in KK-Ay mice, and the increase in urinary protein levels in female KK-Ay mice fed the HFS diet was more pronounced than in *db/db* mice fed the HFS diet. The urinary protein/creatinine ratio also increased in KK-Ay mice. No significant changes were observed in the creatinine clearance levels in any of the groups.

Kidney weights and glomerular size

Absolute kidney weights increased in both diabetic mice, and the kidney weights in male KK-Ay mice were greater than those in male *db/db* mice fed the HFS diet (Fig. 1).

In terms of glomerular size, both the major and minor axes increased in both diabetic mice, and the levels in male *db/db* mice fed the HFS diet were greater than those in the NC diet group (Fig. 2). The increase in glomerular size in female KK-Ay mice fed the HFS diet was greater than that in female *db/db* mice (Fig. 2C and 2D).

Histopathological analyses

Pathological findings in the glomeruli, renal tubules, and tubulointerstitium are shown in Table 5 (male), Table 6 (female) and

Table 1. Biological parameters in male C57BL/6J, *db/db*, and KK-Ay mice at 14 weeks of age

Mouse strain	C57BL/6J		*db/db*		KK-Ay	
Diet	NC	HFS	NC	HFS	NC	HFS
Body weight (g)	27.3 ± 0.8	31.8 ± 3.4	45.5 ± 1.6**	53.9 ± 3.8**, ††	49.2 ± 3.5**	53.4 ± 3.0**
Glucose (mg/dL)	276 ± 13	303 ± 44	904 ± 52**	922 ± 154**	630 ± 29**	833 ± 95**, ††
Insulin (ng/mL)	0.53 ± 0.19	1.56 ± 1.17	3.02 ± 1.05	1.04 ± 0.55	14.5 ± 6.51**	8.69 ± 5.17*, #
Triglyceride (mg/dL)	54.1 ± 16.9	121.6 ± 78.9	317.0 ± 167.0	191.5 ± 82.9	611.5 ± 199.3**	633.1 ± 265.2**, ##
Total cholesterol (mg/dL)	82.5 ± 7.6	154.9 ± 15.9††	166.4 ± 10.4**	318.6 ± 34.5**, ††	180.1 ± 12.1**	214.4 ± 16.2**, †, ##
Urine volume (mL/8 hr)	0.22 ± 0.13	0.22 ± 0.21	2.72 ± 1.57*	3.21 ± 1.77*	0.59 ± 0.41	1.82 ± 1.47
Urine protein (mg/8 hr)	0.79 ± 0.31	1.02 ± 0.98	1.45 ± 0.86	3.32 ± 2.04	2.83 ± 2.18	4.98 ± 2.20*
Urine protein/creatinine ratio	0.012 ± 0.002	0.014 ± 0.004	0.010 ± 0.004	0.016 ± 0.007	0.039 ± 0.012**	0.041 ± 0.016##
Creatinine clearance (mL/hr*g)	0.38 ± 0.25	0.31 ± 0.24	0.47 ± 0.23	0.66 ± 0.28	0.20 ± 0.13	0.37 ± 0.25

Data represent means ± SD (n=4–5). *$P<0.05$, **$P<0.01$; significant difference between C57BL/6J mice and *db/db* or KK-Ay mice in each diet. †$P<0.05$, ††$P<0.01$; significant difference between normal chow (NC) diet and high-fat/high-sucrose (HFS) diet in each strain. #$P<0.05$, ##$P<0.01$; significant difference between *db/db* mice fed HFS diet and KK-Ay mice fed HFS diet.

Table 2. Individual raw data of urine creatinine and serum creatinine in male C57BL/6J, *db/db*, and KK-Ay mice at 14 weeks of age

Animal number	Urine creatinine (mg/dL)						Serum creatinine (mg/dL)					
	C57BL/6J		*db/db*		KK-Ay		C57BL/6J		*db/db*		KK-Ay	
	NC	HFS	NC	HFS	NC	HFS	NC	HFS	NC	HFS	NC	HFS
1	59.60	27.20	7.17	5.43	26.83	18.78	0.12	0.08	0.12	0.12	0.10	0.10
2	36.35	42.20	5.25	8.45	9.64	32.83	0.10	0.12	0.08	0.02	0.10	0.10
3	35.32	40.48	9.91	5.51	22.45	20.92	0.10	0.10	0.06	0.04	0.08	0.16
4	26.00	52.70	4.77	5.05	6.02	14.12	0.06	0.10	0.10	0.06	0.10	0.08
5	26.95	58.10	3.75	11.56	13.26	11.44	0.08	0.08	0.08	0.08	0.14	0.12

NC; normal chow diet, HFS; high-fat/high-sucrose diet.

Table 3. Biological parameters in female C57BL/6J, *db/db*, and KK-Ay mice at 14 weeks of age

Mouse strain	C57BL/6J		*db/db*		KK-Ay	
Diet	NC	HFS	NC	HFS	NC	HFS
Body weight (g)	21.5 ± 1.5	22.5 ± 1.6	48.7 ± 4.4**	58.2 ± 2.0**, ††	53.8 ± 5.0**	63.6 ± 4.8**, ††
Glucose (mg/dL)	196 ± 16	237 ± 22	897 ± 48**	986 ± 176**	554 ± 168**	705 ± 75**, ##
Insulin (ng/mL)	0.70 ± 0.37	0.58 ± 0.10	1.98 ± 1.94	1.33 ± 0.72	124.2 ± 45.3**	43.3 ± 23.6*, ††, #
Triglyceride (mg/dL)	31.0 ± 18.8	26.9 ± 19.3	303.0 ± 53.3	198.9 ± 127.0	458.9 ± 75.8	1,324.3 ± 546.9**, ††, ##
Total cholesterol (mg/dL)	70.5 ± 5.8	105.0 ± 8.2	154.2 ± 13.0*	256.5 ± 43.0**, ††	213.1 ± 32.8**	312.6 ± 69.2**, ††
Urine volume (mL/8 hr)	0.29 ± 0.19	0.16 ± 0.12	2.52 ± 2.04*	3.21 ± 0.66**	1.55 ± 0.29	3.44 ± 0.97**
Urine protein (mg/8 hr)	0.35 ± 0.30	0.24 ± 0.13	0.45 ± 0.34	1.05 ± 0.29	5.29 ± 4.1*	10.85 ± 5.0**, ##
Urine protein/creatinine ratio	0.004 ± 0.001	0.003 ± 0.000	0.003 ± 0.002	0.003 ± 0.002	0.028 ± 0.016*	0.036 ± 0.019**, ##
Creatinine clearance (mL/hr*g)	0.42 ± 0.36	0.27 ± 0.16	0.49 ± 0.29	0.47 ± 0.30	0.32 ± 0.06	0.32 ± 0.06

Data represent means ± SD (n=4–5). *P<0.05, **P<0.01; significant difference between C57BL/6J mice and *db/db* or KK-Ay mice in each diet. ††P<0.01; significant difference between normal chow (NC) diet and high-fat/high-sucrose (HFS) diet in each strain. #P<0.05, ##P<0.01; significant difference between *db/db* mice fed HFS diet and KK-Ay mice fed HFS diet.

Table 4. Individual raw data of urine creatinine and serum creatinine in female C57BL/6J, *db/db*, and KK-Ay mice at 14 weeks of age

Animal number	Urine creatinine (mg/dL)						Serum creatinine (mg/dL)					
	C57BL/6J		*db/db*		KK-Ay		C57BL/6J		*db/db*		KK-Ay	
	NC	HFS	NC	HFS	NC	HFS	NC	HFS	NC	HFS	NC	HFS
1	12.70	29.90	5.00	22.50	15.40	20.10	0.16	0.16	No data	0.12	0.12	0.16
2	34.70	34.10	5.70	6.00	12.60	23.70	0.12	0.12	0.12	0.16	0.16	0.12
3	38.10	24.70	4.80	8.30	10.80	17.40	0.12	0.16	0.12	0.08	0.12	0.24
4	23.20	26.60	8.60	6.40	12.80	30.30	0.16	0.16	0.04	0.12	0.20	0.20
5	35.40	No data	6.20	7.20	14.60	25.80	0.12	0.20	0.16	0.16	0.16	0.24

NC; normal chow diet, HFS; high-fat/high-sucrose diet.

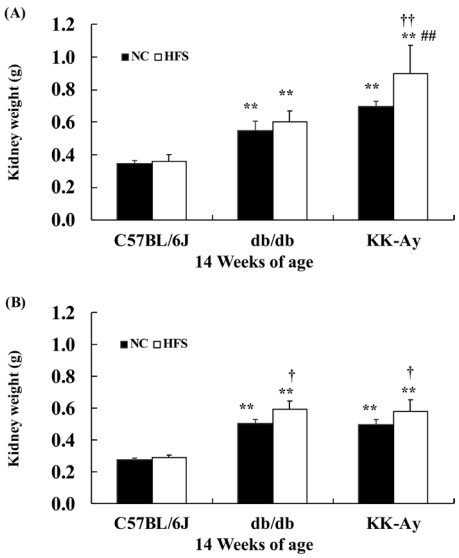

Fig. 1. Kidney weights of 14-week-old C57BL/6J, *db/db*, and KK-Ay mice. Kidney weight in male (**A**) and female (**B**) mice. Data are presented as means ± SD (n=5). **P<0.01; significant difference between C57BL/6J mice fed normal chow (NC) diet and *db/db* or KK-Ay mice. †P<0.05, ††P<0.01; significant difference between NC diet and high-fat/high-sucrose (HFS) diet in each strain. ##P<0.01; significant difference between *db/db* mice fed HFS diet and KK-Ay mice fed HFS diet.

Fig. 3 (HE and SR staining). Regarding glomerular results, very slight changes (±) of mesangial hyperplasia and fibrosis were observed in male *db/db* mice fed the HFS diet and KK-Ay mice fed both diets. Very slight changes (±) of glomerular hypertrophy were also observed in KK-Ay mice.

Renal tubular changes, such as regeneration, tubular dilation, urinary cast, and Armanni-Ebstein lesion, were observed in both diabetic mice as a grade of very slight (±) to moderate (2+) and more frequently observed in KK-Ay mice.

Tubulointerstitial changes, such as infiltration inflammatory cell and fibrosis, were observed in KK-Ay mice fed the HFS diet with a grade of very slight (±) or slight (+) and KK-Ay mice fed the NC diet also showed very slight changes of fibrosis; however, tubulointerstitial lesions were not observed in *db/db* mice.

Lipid accumulation in the kidney was evaluated by Oil Red O staining (Fig. 4). In C57BL/6J mice, no lipid accumulation was observed in either the NC diet or the HFS diet. In *db/db* mice, lipid accumulation was observed in all staining samples, and the lipids accumulated in the macula densa and tubules. In KK-Ay mice, lipid accumulation was observed in two out of five mice fed the NC diet and in all mice fed the HFS diet. The lipid accumulation was observed in the glomeruli of the KK-Ay mice. This lipid accumulation deteriorated with the HFS diet.

Renal mRNA expression

The mRNA levels of fibrotic genes, such as TGF-β and TIMP-1 in the kidney were measured. The TGF-β mRNA levels were tended to increase in male diabetic mice fed the HFS diet (Fig. 5A). TIMP-1 mRNA levels increased or tended to increase in male and female KK-Ay mice, and the increase in TIMP-1 mRNA levels in male mice was enhanced by the HFS diet (Fig. 5B).

DISCUSSION

DKD develops in approximately 40% of the patients with diabetes and is a common cause of ESRD [5, 28]. Some patients with DKD progress to ESRD despite adequate multifactorial treatment, including diet therapies and glycemic, lipid, and

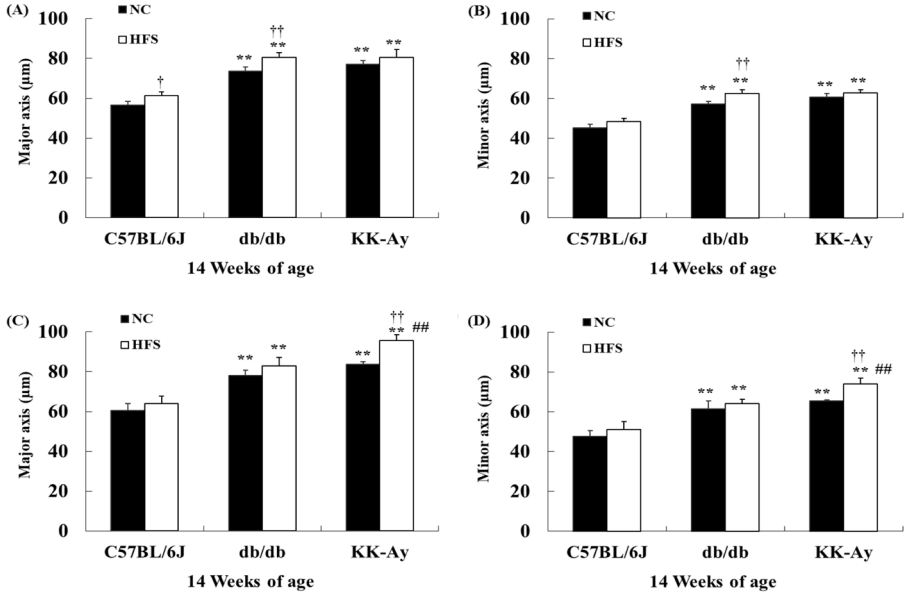

Fig. 2. Glomerular size of 14-week-old C57BL/6J, *db/db*, and KK-Ay mice. Major (**A**) and minor (**B**) axis in male mice. Major (**C**) and minor (**D**) axis in female mice. Data are presented as means ± SD (n=5). ***P*<0.01; significant difference between C57BL/6J mice fed normal chow (NC) diet and *db/db* or KK-Ay mice. †*P*<0.05, ††*P*<0.01; significant difference between NC diet and high-fat/high-sucrose (HFS) diet in each strain. ##*P*<0.01; significant difference between *db/db* mice fed HFS diet and KK-Ay mice fed HFS diet.

Table 5. Histopathological findings in kidney of male C57BL/6J, *db/db*, and KK-Ay mice at 14 weeks of age

Strain	C57BL/6J										*db/db*										KK-Ay									
Diet	NC					HFS					NC					HFS					NC					HFS				
Animal No.	1	2	3	4	5	6	7	8	9	10	11	12	13	14	15	16	17	18	19	20	21	22	23	24	25	26	27	28	29	30
Glomeruli																														
Hypertrophy	–	–	–	–	–	–	–	–	–	–	–	–	–	–	–	–	–	–	–	–	±	–	–	–	–	±	–	–	–	–
Mesangial hyperplasia	–	–	–	–	–	–	–	–	–	–	–	–	–	–	–	–	±	–	–	–	–	–	–	±	–	±	–	±	–	±
Fibrosis	–	–	–	–	–	–	–	–	–	–	–	–	–	–	–	–	–	–	–	±	–	–	–	–	–	–	–	–	±	–
Renal tubule																														
Regeneration	–	–	–	–	–	–	–	–	–	–	–	–	–	–	±	–	±	–	–	–	±	–	–	+	±	±	±	–	–	±
Tubular dilatation	–	–	–	–	–	–	–	–	–	–	–	–	–	–	–	–	–	–	–	–	±	–	–	±	±	±	–	±	–	±
Urinary cast	–	–	–	–	–	–	–	–	–	–	–	–	–	–	±	–	–	–	–	–	±	–	–	+	±	±	–	±	–	±
Armanni-Ebstein lesion	–	–	–	–	–	–	–	–	–	–	–	–	–	–	–	–	±	±	2+	–	±	–	+	±	±	±	–	–	–	–
Tubulointerstitium																														
Infiltration inflammatory cell	–	–	–	–	–	–	–	–	–	–	–	–	–	–	–	–	–	–	–	–	–	–	–	–	–	–	±	±	±	–
Fibrosis	±	–	–	–	–	–	±	–	–	–	–	–	–	–	–	–	–	–	–	–	–	–	–	±	±	–	±	±	+	±

Grades of severity for findings: negative (−), very slight (±), slight (+), or moderate (2+). NC; normal chow, HFS; high-fat/high-sucrose.

Table 6. Histopathological findings in kidney of female C57BL/6J, *db/db*, and KK-Ay mice at 14 weeks of age

Strain	C57BL/6J										*db/db*										KK-Ay									
Diet	NC					HFS					NC					HFS					NC					HFS				
Animal No.	1	2	3	4	5	6	7	8	9	10	11	12	13	14	15	16	17	18	19	20	21	22	23	24	25	26	27	28	29	30
Glomeruli																														
Hypertrophy	–	–	–	–	–	–	–	–	–	–	–	±	–	–	–	–	–	–	–	–	–	–	–	–	–	±	±	–	–	–
Mesangial hyperplasia	–	–	–	–	–	–	–	–	–	–	–	–	–	–	–	–	–	–	–	–	–	–	–	±	–	–	–	–	–	–
Fibrosis	–	–	–	–	–	–	–	–	–	–	–	–	–	–	–	–	–	–	–	–	–	±	–	–	–	–	±	±	±	–
Renal tubule																														
Regeneration	–	–	–	–	–	–	–	–	–	–	–	–	–	–	–	–	–	–	–	–	–	±	–	±	–	–	+	–	+	–
Tubular dilatation	–	–	–	–	–	–	–	–	–	–	–	–	–	–	–	–	–	–	–	–	–	±	–	±	–	–	±	±	±	±
Urinary cast	–	–	–	–	–	–	–	–	–	–	–	–	–	–	–	±	–	–	–	–	–	+	+	±	–	–	+	+	±	±
Armanni-Ebstein lesion	–	–	–	–	–	–	–	–	–	–	–	–	±	–	–	–	–	–	–	–	–	–	–	–	–	–	+	–	±	±
Tubulointerstitium																														
Infiltration inflammatory cell	–	–	–	–	–	–	–	–	–	–	–	–	–	–	–	–	–	–	–	–	–	–	–	–	–	–	–	±	–	–
Fibrosis	±	–	–	–	–	–	±	–	–	–	–	–	–	–	–	–	–	–	–	–	–	±	–	–	–	–	±	±	±	–

Grades of severity for findings: negative (−), very slight (±), slight (+), or moderate (2+). NC; normal chow, HFS; high-fat/high-sucrose.

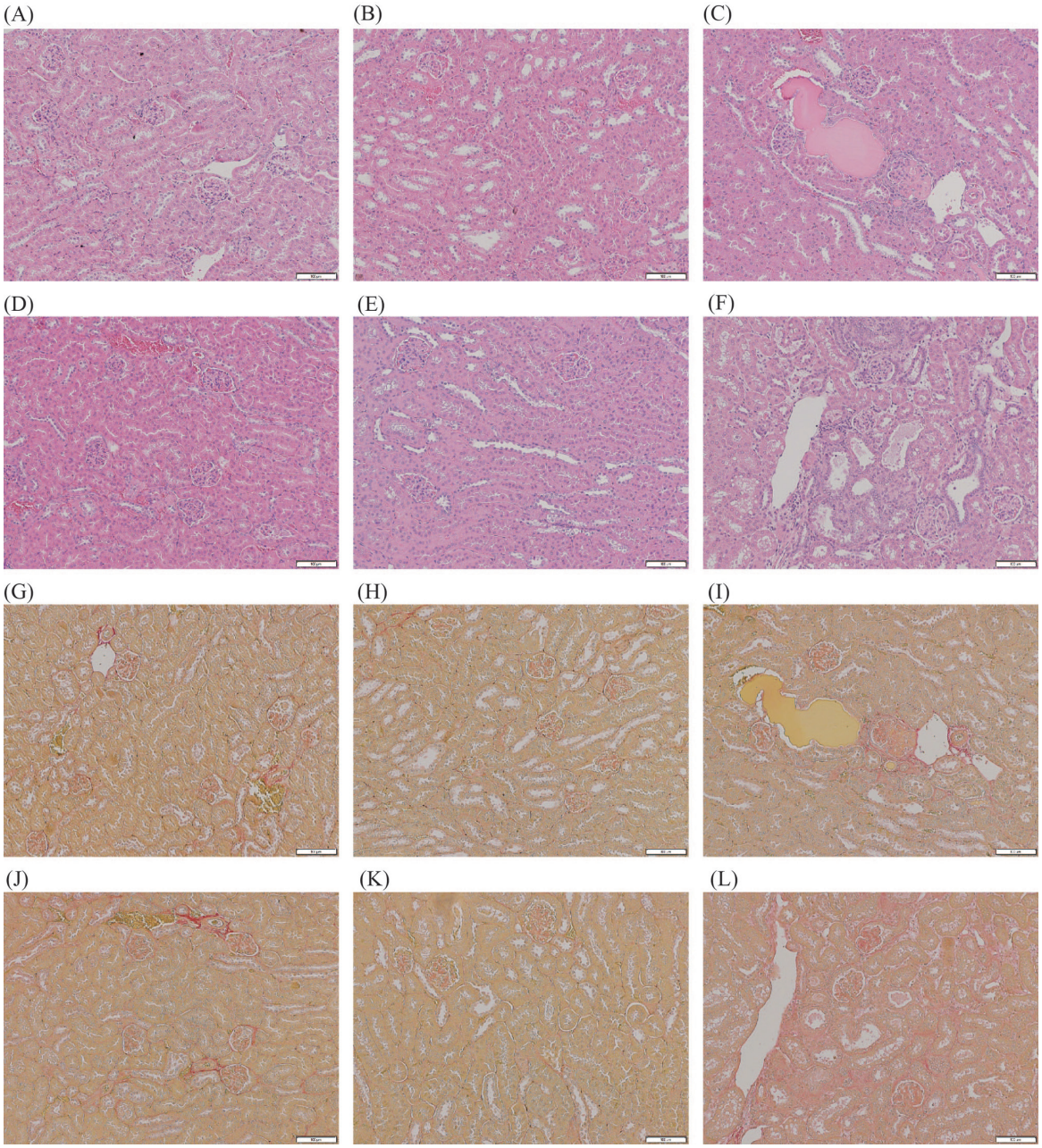

Fig. 3. Histological representative images of 14-week-old male C57BL/6J, *db/db*, and KK-Ay mice. (A)–(F) HE staining, (G)–(L) SR staining. (**A**, **G**) C57BL/6J mice fed normal chow (NC) diet (Animal No. 1). (**B**, **H**) *db/db* mice fed NC diet (Animal No. 11). (**C**, **I**) KK-Ay mice fed NC diet (Animal No. 24). (**D**, **J**) C57BL/6J mice fed high-fat/high-sucrose (HFS) diet (Animal No. 6). (**E**, **K**) *db/db* mice fed HFS diet (Animal No. 20). (**F**, **L**) KK-Ay mouse fed HFS diet (Animal No. 29). Bar=100 µm.

blood pressure control by drug therapies [15, 20]. Therefore, novel and beneficial therapies for DKD must be developed. Animal models are important for elucidating the pathogenesis of diseases and developing new therapies, and are essential for further advancement in disease research, including nephrology. Many animal models of diabetes have been established to study diabetic complications including DKD [12, 16, 34].

In the present study, we investigated the pathophysiological features of *db/db* and KK-Ay mice fed a HFS diet. Tubulointerstitial fibrosis, a common pathway in CKD, has not been observed in *db/db* and KK-Ay mice fed a standard diet [16]. Both *db/db* and KK-Ay mice showed glucose/lipid metabolism abnormalities, and KK-Ay mice showed marked hyperinsulinemia, suggesting the development of strong insulin resistance. The blood glucose levels of *db/db* mice were higher than those of KK-Ay mice, but isoflurane anesthesia has an elevating effect on blood glucose levels [7], and the background of these blood glucose levels must be carefully considered. In another preliminary study, the blood glucose level of unanesthetized *db/db* mice was approximately 480 mg/dL (mean value of four 16-week-old mice). The HFS diet tended to worsen renal parameters, as indicated by changes in urine volume and urinary protein. In male *db/db* and KK-Ay mice fed the HFS diet, creatinine clearance increased, suggesting modulation of renal function.

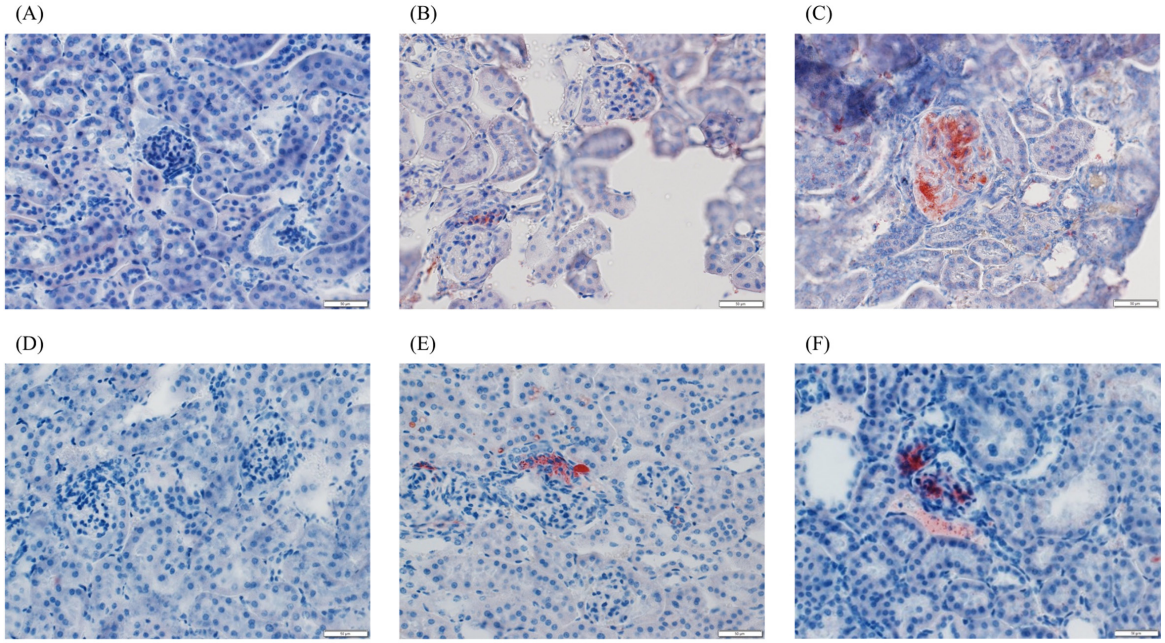

Fig. 4. Histological representative images of 14-week-old male C57BL/6J, *db/db*, and KK-Ay mice. (**A**) C57BL/6J mice fed normal chow (NC) diet (Animal No. 1). (**B**) *db/db* mice fed NC diet (Animal No. 11). (**C**) KK-Ay mice fed NC diet (Animal No. 24). (**D**) C57BL/6J mice fed high-fat/high-sucrose (HFS) diet (Animal No. 6). (**E**) *db/db* mice fed HFS diet (Animal No. 20). (**F**) KK-Ay mouse fed HFS diet (Animal No. 29). Oil red O staining, bar=50 µm.

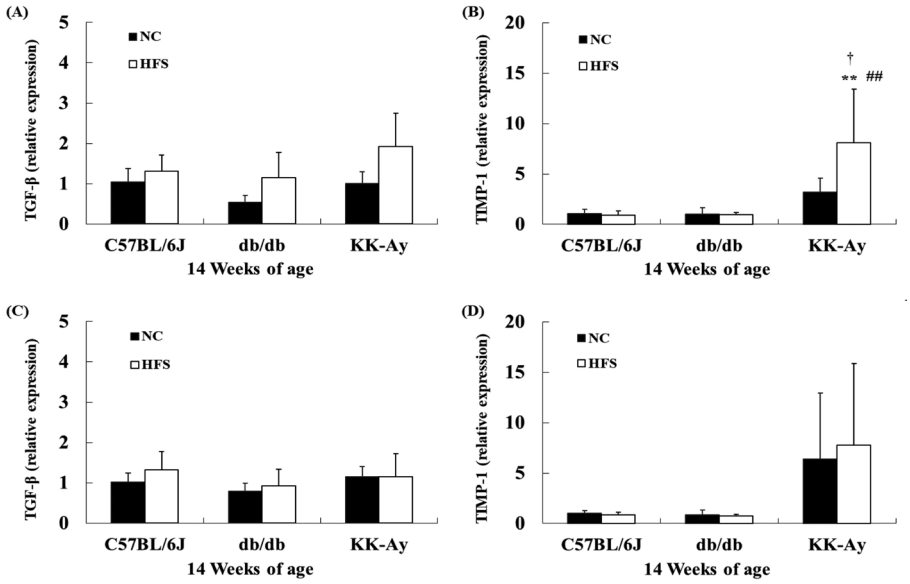

Fig. 5. mRNA expression of renal genes related to fibrosis in 14-week-old C57BL/6J, *db/db*, and KK-Ay mice. (**A**) TGF-β and (**B**) TIMP-1 expression in male mice. (**C**) TGF-β and (**D**) TIMP-1 expression in female mice. Data are presented as means ± SD (n=5). $^{**}P<0.01$; significant difference between C57BL/6J mice fed normal chow (NC) diet and *db/db* or KK-Ay mice. $^{\dagger}P<0.05$; significant difference between NC diet and high-fat/high-sucrose (HFS) diet in each strain. $^{\#\#}P<0.01$; significant difference between *db/db* mice fed HFS diet and KK-Ay mice fed HFS diet. TGF-β; transforming growth factor-β, TIMP-1; tissue inhibitor of metalloproteinase-1.

In pathological analyses, morphological changes such as renal hypertrophy and an increase in glomerular size were observed in both diabetic mice, and these changes were enhanced by the HFS diet. Hypercholesterolemia was enhanced by the HFS diet. Cholesterol is a macronutrient that contributes to the development and progression of renal diseases [3, 13, 43]. Hypercholesterolemia adversely affects cellular functions and signaling pathways, including mitochondrial function and hypoxic and inflammatory response [41].

Histopathological findings in the glomeruli, renal tubules, and/or tubulointerstitium were observed in both diabetic mice, and both the severity and frequency of the lesions were clearly stronger in KK-Ay mice than in *db/db* mice. Moreover, all lesions were more clearly observed in the male mice than in the female mice. Tubulointerstitial fibrosis was clearly observed in KK-Ay mice fed the HFS diet; however, fibrosis changes were not observed in *db/db* mice. Because hyperinsulinemia was more significant in KK-Ay mice than in *db/db* mice, strong insulin resistance in KK-Ay mice may contribute to the development and progression of tubulointerstitial fibrosis. Increased insulin resistance increases the secretion of inflammatory factors from adipose tissue, which can lead to the accumulation of ectopic fat [4], thereby causing renal damage through increased endoplasmic reticulum stress and oxidative stress. Actually, an increase

in fat accumulation in the glomeruli showed a similar tendency to increase of tubulointerstitial fibrosis. People with insulin resistance are more likely to develop renal complications [1]. Hyperinsulinemia induces inappropriate dilation of afferent arterioles, resulting in glomerular and tubular lesions [17]. It has also been reported that the HFS diet increases blood pressure [18], and hemodynamic abnormalities due to hypertension may be involved in these lesions. The pathological evaluation of glomeruli is presented as the ratio of the number of abnormal glomeruli to the total number of glomeruli, and is limited in that it does not assess the severity of each glomerulus. It has also been reported that interstitial fibrosis is promoted when renal tubular lesions are severe [38], and tubular lesions are clearly stronger in KK-Ay mice. Moreover, leptin is reportedly associated with development and progression in hepatic fibrosis [23]. The leptin receptor in renal tubular cells plays a key role for the response to diet-induced hyperleptinemia and obesity including albuminuria [14]. Leptin signaling is impaired in *db/db* mice and interstitial fibrosis may not be observed in *db/db* mice. Crosstalk between insulin and leptin signaling has also been reported, and attenuation of insulin signaling leads to enhancement of leptin signaling [37]. Hyperinsulinemia in KK-Ay mice may further enhance leptin signaling. The progression of DKD is thought to involve a complex combination of insulin signaling, leptin signaling, lipid metabolism, and other factors, but these results suggest that abnormalities in insulin signaling are a particularly important factor. There is a discrepancy between the incidence of glomerular size measurements (Fig. 2) and glomerular pathological findings including hypertrophy and mesangial hyperplasia (Table 5 and 6). It is possible that the amount of change in glomerular size is not large, but this discrepancy needs to be investigated in future studies with a longer period.

Pathological lipid accumulation in the glomeruli is one of the prominent features in DKD and the lipotoxicity is closely related to the onset and progression of DKD [11, 44]. Lipid accumulation in podocytes plays a key role in development of DKD, and the glomerular lipid accumulation is a potential therapeutic target in DKD [11]. Moreover, lipid droplet deposition in the kidney of *db/db* mice is reportedly increased compared to that in C57BL/KSJ mice [45]. Interestingly, the lipid accumulation sites in the kidneys were different from *db/db* mice (macula densa) and KK-Ay mice (glomeruli). Tubulointerstitial fibrosis in KK-Ay mice may be enhanced by glomerular lipid accumulation via a HFS diet. Furthermore, the diet appears to increase glomerulus fat accumulation with prolonged administration. Tubulointerstitial damage is closely correlated with glomerular damage in renal disease models [30, 39], and abnormal protein filtration induces the progression of renal damage toward interstitial fibrosis and glomerular sclerosis [46].

In conclusion, differences in pathological changes in response to a HFS diet were observed between *db/db* and KK-Ay mice. The diet exacerbated renal lesions with tubulointerstitial fibrosis in KK-Ay mice, suggesting its usefulness as a DKD model.

CONFLICT OF INTEREST. Chika Oki and Tomohiko Sasase are employees of Japan Tobacco Inc. Masami Shinohara is an employee of CLEA Japan, Inc. Kinuko Uno, Takahiro Tsutsui, Keita Sekiguchi, Ayane Yamaguchi, Kouhei Mandai, Miki Sugimoto, Tatsuya Maekawa, Katsuhiro Miyajima, and Takeshi Ohta have no conflict of interest in relation to this study.

ACKNOLEDGMENTS. We wish to thank Ms. Fuko Kuroki, Ms. Mei Nishida, Mr. Tomoki Ogo (Kyoto University, Graduate School of Agriculture), Mr. Masaaki Handa, and Mr. Yoshinobu Doi (CLEA Japan) for their long-term animal care and study support.

REFERENCES

1. Ahlqvist E, Storm P, Käräjämäki A, Martinell M, Dorkhan M, Carlsson A, Vikman P, Prasad RB, Aly DM, Almgren P, Wessman Y, Shaat N, Spégel P, Mulder H, Lindholm E, Melander O, Hansson O, Malmqvist U, Lernmark Å, Lahti K, Forsén T, Tuomi T, Rosengren AH, Groop L. 2018. Novel subgroups of adult-onset diabetes and their association with outcomes: a data-driven cluster analysis of six variables. *Lancet Diabetes Endocrinol* **6**: 361–369. [Medline] [CrossRef]
2. Anders HJ, Huber TB, Isermann B, Schiffer M. 2018. CKD in diabetes: diabetic kidney disease versus nondiabetic kidney disease. *Nat Rev Nephrol* **14**: 361–377. [Medline] [CrossRef]
3. Banach M, Aronow WS, Serban MC, Rysz J, Voroneanu L, Covic A. 2015. Lipids, blood pressure and kidney update 2015. *Lipids Health Dis* **14**: 167. [Medline] [CrossRef]
4. Bansal SK, Bansal MB. 2024. Pathogenesis of MASLD and MASH-role of insulin resistance and lipotoxicity. *Aliment Pharmacol Ther* **59** Suppl 1: S10–S22. [Medline] [CrossRef]
5. Cao Z, Cooper ME. 2011. Pathogenesis of diabetic nephropathy. *J Diabetes Investig* **2**: 243–247. [Medline] [CrossRef]
6. Chen H, Charlat O, Tartaglia LA, Woolf EA, Weng X, Ellis SJ, Lakey ND, Culpepper J, Moore KJ, Breitbart RE, Duyk GM, Tepper RI, Morgenstern JP. 1996. Evidence that the diabetes gene encodes the leptin receptor: identification of a mutation in the leptin receptor gene in db/db mice. *Cell* **84**: 491–495. [Medline] [CrossRef]
7. Constantinides C, Mean R, Janssen BJ. 2011. Effects of isoflurane anesthesia on the cardiovascular function of the C57BL/6 mouse. *ILAR J* **52**: e21–e31. [Medline]
8. Dabelea D, Stafford JM, Mayer-Davis EJ, D'Agostino R Jr, Dolan L, Imperatore G, Linder B, Lawrence JM, Marcovina SM, Mottl AK, Black MH, Pop-Busui R, Saydah S, Hamman RF, Pihoker C. SEARCH for Diabetes in Youth Research Group. 2017. Association of type 1 diabetes vs type 2 diabetes diagnosed during childhood and adolescence with complications during teenage years and young adulthood. *JAMA* **317**: 825–835. [Medline] [CrossRef]
9. Feng YL, Wang WB, Ning Y, Chen H, Liu P. 2021. Small molecules against the origin and activation of myofibroblast for renal interstitial fibrosis therapy. *Biomed Pharmacother* **139**: 111386. [Medline] [CrossRef]
10. Fouli GE, Gnudi L. 2019. The future: experimental therapies for renal disease in diabetes. *Nephron* **143**: 3–7. [Medline] [CrossRef]
11. Fu Y, Sun Y, Wang M, Hou Y, Huang W, Zhou D, Wang Z, Yang S, Tang W, Zhen J, Li Y, Wang X, Liu M, Zhang Y, Wang B, Liu G, Yu X, Sun J, Zhang C, Yi F. 2020. Elevation of JAML promotes diabetic kidney disease by modulating podocyte lipid metabolism. *Cell Metab* **32**: 1052–1062.e8. [Medline] [CrossRef]
12. Katsuda Y, Ohta T, Miyajima K, Kemmochi Y, Sasase T, Tong B, Shinohara M, Yamada T. 2014. Diabetic complications in obese type 2 diabetic rat models. *Exp Anim* **63**: 121–132. [Medline] [CrossRef]

13. Keane WF, O'Donnell MP, Kasiske BL, Schmitz PG. 1990. Lipids and the progression of renal disease. *J Am Soc Nephrol* **1** Suppl 2: S69–S74. [Medline]
14. Kim YC, Fattah H, Fu Y, Nespoux J, Vallon V. 2023. Expression of leptin receptor in renal tubules is sparse but implicated in leptin-dependent kidney gene expression and function. *Am J Physiol Renal Physiol* **324**: F544–F557. [Medline] [CrossRef]
15. Kitada M, Kanasaki K, Koya D. 2014. Clinical therapeutic strategies for early stage of diabetic kidney disease. *World J Diabetes* **5**: 342–356. [Medline] [CrossRef]
16. Kitada M, Ogura Y, Koya D. 2016. Rodent models of diabetic nephropathy: their utility and limitations. *Int J Nephrol Renovasc Dis* **9**: 279–290. [Medline] [CrossRef]
17. Knight SF, Imig JD. 2007. Obesity, insulin resistance, and renal function. *Microcirculation* **14**: 349–362. [Medline] [CrossRef]
18. Kobi JBBS, Matias AM, Gasparini PVF, Torezani-Sales S, Madureira AR, da Silva DS, Correa CR, Garcia JL, Haese D, Nogueira BV, de Assis ALEM, Lima-Leopoldo AP, Leopoldo AS. 2023. High-fat, high-sucrose, and combined high-fat/high-sucrose diets effects in oxidative stress and inflammation in male rats under presence or absence of obesity. *Physiol Rep* **11**: e15635. [Medline] [CrossRef]
19. Koya D. 2019. Diabetic kidney disease: its current trends and future therapeutic perspectives. *J Diabetes Investig* **10**: 1174–1176. [Medline] [CrossRef]
20. Koya D, Kitada M, Kume S, Kanasaki K. 2014. Interventions against nutrient-sensing pathways represent an emerging new therapeutic approach for diabetic nephropathy. *Clin Exp Nephrol* **18**: 210–213. [Medline] [CrossRef]
21. Leask A. 2012. CCN3: a novel anti-fibrotic treatment in end-stage renal disease? *J Cell Commun Signal* **6**: 115–116. [Medline] [CrossRef]
22. Lee GH, Proenca R, Montez JM, Carroll KM, Darvishzadeh JG, Lee JI, Friedman JM. 1996. Abnormal splicing of the leptin receptor in diabetic mice. *Nature* **379**: 632–635. [Medline] [CrossRef]
23. Lee KC, Wu PS, Lin HC. 2023. Pathogenesis and treatment of non-alcoholic steatohepatitis and its fibrosis. *Clin Mol Hepatol* **29**: 77–98. [Medline] [CrossRef]
24. Mabrok HB, Ramadan AA, Hamed IM, Mohamed DA. 2024. Obesity as inducer of cognitive function decline via dysbiosis of gut microbiota in rats. *Brain Sci* **14**: 807. [Medline] [CrossRef]
25. Nangaku M. 2006. Chronic hypoxia and tubulointerstitial injury: a final common pathway to end-stage renal failure. *J Am Soc Nephrol* **17**: 17–25. [Medline] [CrossRef]
26. Nie L, Liu Y, Zhang B, Zhao J. 2020. Application of histone deacetylase inhibitors in renal interstitial fibrosis. *Kidney Dis (Basel)* **6**: 226–235. [Medline] [CrossRef]
27. Oshima M, Shimizu M, Yamanouchi M, Toyama T, Hara A, Furuichi K, Wada T. 2021. Trajectories of kidney function in diabetes: a clinicopathological update. *Nat Rev Nephrol* **17**: 740–750. [Medline] [CrossRef]
28. Packham DK, Alves TP, Dwyer JP, Atkins R, de Zeeuw D, Cooper M, Shahinfar S, Lewis JB, Lambers Heerspink HJ. 2012. Relative incidence of ESRD versus cardiovascular mortality in proteinuric type 2 diabetes and nephropathy: results from the DIAMETRIC (diabetes mellitus treatment for renal insufficiency consortium) database. *Am J Kidney Dis* **59**: 75–83. [Medline] [CrossRef]
29. Preibisch S, Saalfeld S, Tomancak P. 2009. Globally optimal stitching of tiled 3D microscopic image acquisitions. *Bioinformatics* **25**: 1463–1465. [Medline] [CrossRef]
30. Sánchez-Lozada LG, Tapia E, Johnson RJ, Rodríguez-Iturbe B, Herrera-Acosta J. 2003. Glomerular hemodynamic changes associated with arteriolar lesions and tubulointerstitial inflammation. *Kidney Int Suppl* (86, Suppl) S9–S14. [Medline] [CrossRef]
31. Sano R, Shinozaki Y, Ohta T. 2020. Sodium-glucose cotransporters: Functional properties and pharmaceutical potential. *J Diabetes Investig* **11**: 770–782. [Medline] [CrossRef]
32. Schneider CA, Rasband WS, Eliceiri KW. 2012. NIH Image to ImageJ: 25 years of image analysis. *Nat Methods* **9**: 671–675. [Medline] [CrossRef]
33. Shinozaki Y, Fukui K, Maekawa M, Toyoda K, Yoshiuchi H, Inagaki K, Uno K, Miyajima K, Ohta T. 2023. Unilateral nephrectomized SHR/NDmcr-cp rat shows a progressive decline of glomerular filtration with tubular interstitial lesions. *Physiol Res* **72**: 209–220. [Medline] [CrossRef]
34. Shinozaki Y, Katayama Y, Yamaguchi F, Suzuki T, Watanabe K, Uno K, Tsutsui T, Sugimoto M, Shinohara M, Miyajima K, Ohta T. 2022. Salt loading with unilateral nephrectomy accelerates decline in glomerular filtration rate in the hypertensive, obese, type 2 diabetic SDT fatty rat model of diabetic kidney disease. *Clin Exp Pharmacol Physiol* **49**: 492–500. [Medline] [CrossRef]
35. Suto J, Matsuura S, Yamanaka H, Sekikawa K. 1999. Quantitative trait loci that regulate plasma lipid concentration in hereditary obese KK and KK-Ay mice. *Biochim Biophys Acta* **1453**: 385–395. [Medline] [CrossRef]
36. Suto J, Matsuura S, Imamura K, Yamanaka H, Sekikawa K. 1998. Genetics of obesity in KK mouse and effects of A(y) allele on quantitative regulation. *Mamm Genome* **9**: 506–510. [Medline] [CrossRef]
37. Takahashi K, Yamada T, Hosaka S, Kaneko K, Asai Y, Munakata Y, Seike J, Horiuchi T, Kodama S, Izumi T, Sawada S, Hoshikawa K, Inoue J, Masamune A, Ueno Y, Imai J, Katagiri H. 2023. Inter-organ insulin-leptin signal crosstalk from the liver enhances survival during food shortages. *Cell Rep* **42**: 112415. [Medline] [CrossRef]
38. Takaori K, Nakamura J, Yamamoto S, Nakata H, Sato Y, Takase M, Nameta M, Yamamoto T, Economides AN, Kohno K, Haga H, Sharma K, Yanagita M. 2016. Severity and frequency of proximal tubule injury determines renal prognosis. *J Am Soc Nephrol* **27**: 2393–2406. [Medline] [CrossRef]
39. Theilig F, Kriz W, Jerichow T, Schrade P, Hähnel B, Willnow T, Le Hir M, Bachmann S. 2007. Abrogation of protein uptake through megalin-deficient proximal tubules does not safeguard against tubulointerstitial injury. *J Am Soc Nephrol* **18**: 1824–1834. [Medline] [CrossRef]
40. Tsuchiya H. 2012. Retinoids as promising treatment for non-alcoholic fatty liver disease. *Yakugaku Zasshi* **132**: 903–909 (in Japanese). [Medline] [CrossRef]
41. Vergara D, Casadei-Gardini A, Giudetti AM. 2019. Oxidative molecular mechanisms underlying liver diseases: from systems biology to the personalized medicine. *Oxid Med Cell Longev* **2019**: 7864316. [Medline] [CrossRef]
42. Wali JA, Ni D, Facey HJW, Dodgson T, Pulpitel TJ, Senior AM, Raubenheimer D, Macia L, Simpson SJ. 2023. Determining the metabolic effects of dietary fat, sugars and fat-sugar interaction using nutritional geometry in a dietary challenge study with male mice. *Nat Commun* **14**: 4409. [Medline] [CrossRef]
43. White SL, Cass A, Atkins RC, Chadban SJ. 2005. Chronic kidney disease in the general population. *Adv Chronic Kidney Dis* **12**: 5–13. [Medline] [CrossRef]
44. Wu M, Yoon CY, Park J, Kim G, Nam BY, Kim S, Park JT, Han SH, Kang SW, Yoo TH. 2024. The role of PCSK9 in glomerular lipid accumulation and renal injury in diabetic kidney disease. *Diabetologia* **67**: 1980–1997. [Medline] [CrossRef]
45. Zheng W, Qian C, Xu F, Cheng P, Yang C, Li X, Lu Y, Wang A. 2021. Fuxin Granules ameliorate diabetic nephropathy in db/db mice through TGF-β1/Smad and VEGF/VEGFR2 signaling pathways. *Biomed Pharmacother* **141**: 111806. [Medline] [CrossRef]
46. Zoja C, Abbate M, Remuzzi G. 2015. Progression of renal injury toward interstitial inflammation and glomerular sclerosis is dependent on abnormal protein filtration. *Nephrol Dial Transplant* **30**: 706–712. [Medline] [CrossRef]